Springer

KSME

Journal of Mechanical Science and Technology 24 (2) (2010) 489~496
www.springerlink.com/content/1738-494x
DOI 10.1007/s12206-010-0104-2

Vision coupled GPS/INS scheme for helicopter navigation †

JaeHyung Kim[1], Joon Lyou[2,*] and HwyKuen Kwak[2]

[1]*Korea Institute of Aerospace Technology, Korean Air, 461-1 Jeonmin-dong, Yuseong-gu, Daejeon 302-811, Korea*
[2]*Dept of Electronics Engineering, Chungnam National University, 220 Gung-dong, Yuseong-gu, Daejeon 305-764, Korea*

(Manuscript Received December 23, 2008; Revised July 2, 2009; Accepted December 29, 2009)

Abstract

This paper presents a framework for a GPS/INS/vision-based helicopter navigation system. The conventional GPS/INS algorithm has weak points such as GPS blockage and jamming, while the helicopter is a speedy and highly dynamic vehicle that may easily lose a GPS signal. A vision sensor is not affected by signal jamming, and the navigation error of such a system does not accumulate. Hence, a GPS/INS/vision-aided navigation scheme was implemented to provide the robust localization suitable for helicopter operations in various environments. The core algorithm is the vision-based SLAM (simultaneous localization and mapping) technique. Flight tests were performed to verify the SLAM-aided vision navigation algorithm. During the tests, it was confirmed that the developed system is sufficiently robust under GPS blockage conditions. The system design, software algorithm, and flight test results are described in this paper.

Keywords: GPS/INS/Vision navigation; SLAM; Kalman filter; Harris corner; SIFT

1. Introduction

1.1 Background and motivation

Inertial navigation units are typically used for aerospace and naval applications [1]. They are able to provide independent navigation solutions and comparably high output rates without external intermediaries. However, the position error of these units accumulates with time. To compensate for this error, an integrated navigation method coupled with other navigation sensors is typically used.

Currently, GPS is mainly used as the other sensor. It provides the position, velocity and time with bounded accuracy. However, GPS is vulnerable to disruptions from several causes, including intentional jamming and atmospheric effects. Especially in a helicopter, owing to the severe attitude variation and the irregular rotation of the main rotor, GPS signal reception properties such as signal attenuation, refraction and diffraction are affected [2]. Consequently, serious problems associated with the performance of the overall navigation system occur, and therefore an auxiliary sensor in addition to GPS for a more stable and accurate system is required that is applicable in spite of jamming, noise and other detrimental factors.

Recent studies related to visual information in self-motion and tracking have looked at the ability to estimate attitude and distance. Vision systems are currently used in navigation to provide error compensation to a conventional GPS/INS navigation system.

1.2 Related work

In recent years, vision sensors have attracted the attention of many researchers as they are a good source of information [3, 4, 5]. Additionally, related algorithms pertaining to the optic flow and feature point have been the subject of in-depth studies.

Improving the accuracy in vision-based navigation depends on the image tracking performance. Recent developments related to the detection of keypoints in images have led to navigation solutions that are more accurate. Various SLAM algorithms based on SIFT features were proposed by Lowe [6]. In these algorithms, the features are invariant to image scaling and rotation, and partially invariant to changes in the 3D viewpoint, added noise, and changes in illumination. This contrasts to the Harris corner detector [7].

As for vision-based approaches to navigation, Ettinger [8] presents a vision-guided flight stability and autonomy system that is based on a robust horizon detection algorithm. Horizon detection methods are limited in that the horizon must be in view, and they can only resolve pitch and roll and not yaw. The optical flow approach has been used to estimate the depth of an antonymous take-off and landing, as well as for collision avoidance [9].

† This paper was recommended for publication in revised form by Associate Editor Kyongsu Yi

*Corresponding author. Tel.: +82 42 821 5669, Fax.: +82 42 823 5436
E-mail address: jlyou@cnu.ac.kr

SLAM-aided vision navigation for an airborne system has been implemented with monocular vision in combination with accurate inertial sensors [10]. A vision camera is used to compute the bearing and depth of each feature. The available range information improves the position accuracy and stability of the SLAM solution. However, the targets are artificially placed and this approach based on a single camera is limited in terms of collecting the information necessary to estimate the 6-dof depth of the features. As for helicopter navigation, this method has weak points in that it is easy to miss the feature point owing to the fast dynamics of a helicopter.

1.3 Our work

Recent advances in image-processing technologies are opening the door to a new method of integrated navigation utilizing GPS, INS and vision sensors. Due to the capability of flight vehicles to move freely in a 3D space, a single-camera-based approach is limited in how it estimates the position and attitude of a vehicle due to the narrow field of view (FOV) of an image sensor compared to a wide natural scene.

Therefore, for better coverage of the natural scene and to allow information extraction from the image, a methodology using two cameras is proposed. The first camera is forward-facing, and the second faces downward. The forward camera is mainly in charge of attitude correction by estimating the line-of-sight from the vehicle to the forward-looking feature point. The downward-facing camera is mainly for position correction by measuring the displacement variance that occurs while the vehicle is moving.

This paper presents various results using multi-vision sensor data in a GPS/INS system, including information related to coupling the information from two cameras and implementing a practical SLAM system to build a map within an unknown environment while at the same time estimating positions inside the map. We also show a proposed GPS/INS/Vision navigation system uses the position and gimbal angle information from the vision sensors for the error compensation to the conventional GPS/INS navigation system.

2. System description

The system can be broken down into five distinct components: a navigation system, two vision processors, a tactical information processor and a display device, as shown in Fig. 1. The navigation system based on NDGPS/INS provides the position, attitude and reliability data to the tactical information processor(TIP) via a RS-422 port. TIP has detailed terrain data of all of South Korea including digital elevation model (DEM) data as well as satellite imagery for elaborate artificial vision. Therefore, it can provide a pilot with an artificial view that is similar to an actual view from an external cockpit.

2.1 Navigation system

The navigation System consists of a beacon receiver, GPS receiver, IMU (inertial measurement unit), and processor

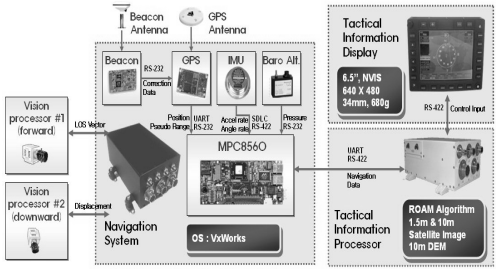

Fig. 1. Block diagram of the GPS/INS/vision system.

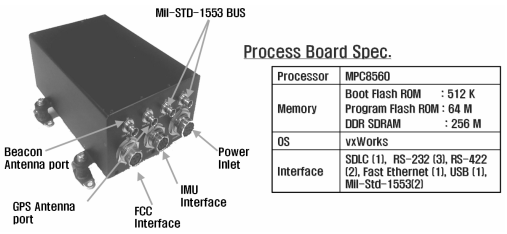

Fig. 2. Specification of the navigation board.

board, as shown in Fig. 2.

The MPC8560 PowerQUICC III processor is based on Freescale's e500 system, with a maximum clock speed of up to 1GHz and a 64bit interface RISC (reduced instruction set computing) chip [11]. The performance of MPC8560 is capable of sufficiently running navigation algorithms as well as gathering and processing all of the information from the GPS receiver, the IMU, and other sensors simultaneously.

2.2 Tactical information processor

The goal is to render all of the satellite images (maximum.0.7m resolution) and DEM data (10m) of South Korea. However, it is not easy to render a large volume of terrain data at a high resolution in real time. As the size of the terrain data increases, it becomes increasingly difficult to process all of the data in the main memory during the visualization process.

Thus, data exchanges between the main memory and secondary storage were utilized. This eventually became a bottleneck in terrain visualization. To prevent the slowdown of the visualization performance, a modified ROAM (real-time optimally adapting meshes) algorithm is used. This algorithm is a type of large terrain level-of-detail technique that works with large terrain models and allows them to be rendered in real time [12].

2.3 Tactical information display

The tactical information display device is a 6.5-inch 640X480 flat panel display that supports the function of night vision imaging system and complies with the most hostile specifications regarding shock, vibration, temperature and electromagnetic compatibility, as shown in Fig. 3. Functions provided by the multi function display(MFD) include display

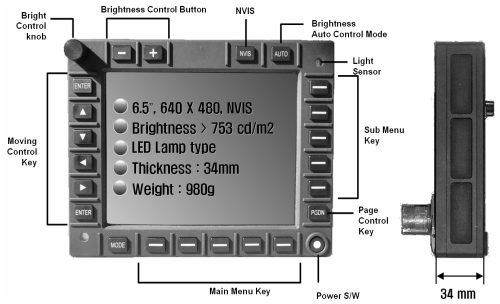

Fig. 3. Specification of the tactical information display.

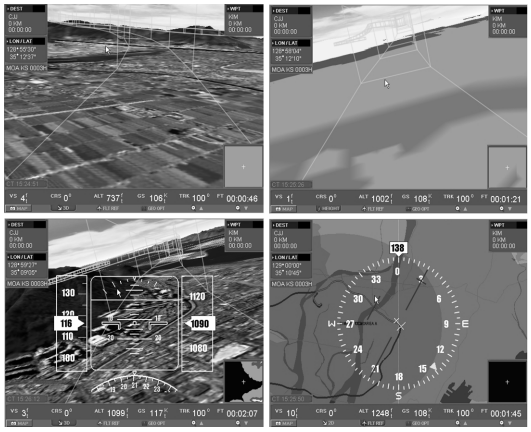

Fig. 4. Tactical information displays.

of the attitude, speed, air data, airframe status, airport information, terrain, as well as obstacle alerting, situational awareness via a 2D moving map display, and 3D artificial vision. In addition, the display device is controlled by knobs and selector keys located on the MFD bezels.

Fig. 4 shows a pathway-in-the-sky [13] view, a height map view, and major aircraft instruments including the vertical situation indicator(VSI) and the horizontal situation indicator(HSI). VSI provides the aircraft heading, altitude, ground speed, roll and yaw, while HSI provides the track angle and the aircraft heading.

3. System modeling

3.1 Structure of navigation software

Fig. 5 and Table 1 show the function of the navigation algorithm. The position variance and line-of-sight(LOS) information calculated from the image sensor are integrated into the SLAM-aided GPS/INS/vision Kalman filter, and the error is compensated by comparing the difference between the estimated feature point by a Kalman filter and the point of image coordinates calculated by measurement model.

Two cameras that form a 90 degree angle are perpendicular to each other and observe the forward and downward feature point, respectively. To capture images from the downward-looking camera, the direct geo-referencing method is used. This method can provide a coordinate solution on an arbitrary

Table 1. Vision-based algorithm comparison.

Classification	Forward	Downward
Image processing	SIFT (refer to Fig. 15)	Harris Corner (refer to Fig. 16)
Algorithm	Line of Sight (LOS)	Direct Geo-referencing
Distance Calculation	LOS and DEM	Radio Altitude and Aircraft Attitude
Processing Rate	4 Hz	10 Hz
Compensation	Attitude (Heading)	Position (2D)

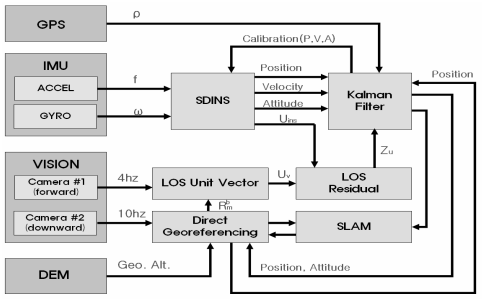

Fig. 5. Block diagram of the present navigation algorithm.

feature on 3D space and can also calculate the current 3D position of a moving vehicle from a known feature point. From the image of the forward-looking camera, it provides the LOS residual from the two types of measurement into the Kalman filter. The first of these measurements is from the gimbal angle calculated by the forward-looking image and an inertial sensor, and the second is from the position of the vehicle to an arbitrary landmark.

As a result, this multi-vision-based approach can obtain better error compensation compared to a direct geo-referencing method that only uses a downward-looking image. Moreover, it can obtain solutions that are more accurate compared to those of the single-vision-based approach.

To provide a precise position and attitude calculation using direct geo-referencing and LOS, it is necessary to know the precise altitude of the aircraft relative to the surface of the Earth. To do this, the data from the radio altitude, barometric altitude and GPS altitude are used to estimate the precise altitude of the aircraft.

3.2 Direct geo-referencing method

The direct geo-referencing method is a technique that converts the image point of the lens on the camera to the exterior orientation elements, as shown in Table 2 and Fig. 6. It is used to provide a solution for unknown feature points on the Earth's surface or alternatively provide the position of a vehicle from known feature points on the Earth's surface through a coordinate transformation of the image, camera, the inertial and the reference coordinates [14, 15].

$$r_p^m(t) = r_{GPS}^m(t) + C_b^m(t)(s_c \cdot C_c^b \cdot r_p^c - a_{INS}^c - a_{INS}^{GPS}) \quad (1)$$

Table 2. Terms in the direct geo-referencing equation.

Variable	Description
r_p^m	Position point vector of interest represented in the mapping frame
r_{INS}^m , r_{GPS}^m	Position of navigation sensor point vector of interest represented in the mapping frame
s_c	Scale factor between the image space and the object space
C_b^m	Rotation matrix between the IMU body frame and the mapping frame
C_c^b	Rotation matrix between the image frame and the IMU body frame
r_p^c	Location of the point of interest represented in the image frame
a_{INS}^c	Lever arm offset between the IMU body frame and the image frame
a_{INS}^{GPS}	Lever arm offset between the IMU body frame and the GPS antenna

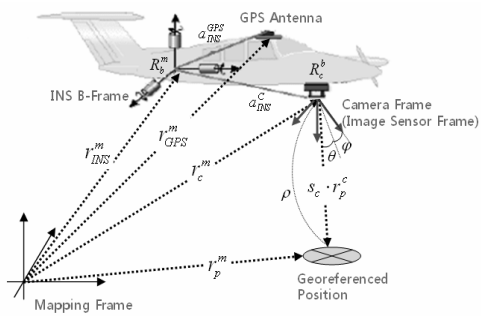

Fig. 6. Concept of direct georeferencing model [14].

where $r_{GPS}^m(t)$ and $C_b^m(t)$ is the position and attitude information determined by GPS/INS navigation system, and it is the time dependent exterior element. C_c^b , a_{INS}^b , a_{INS}^{GPS} is the offset and boresight angle between camera and inertial sensor coordinate and also the exterior element determined by angle calibration among the mounted equipment.

Factors influencing the accuracy of direct geo-referencing include the position of the vehicle and its attitude, the boresight measurement, the lever arm offset and the displacement of the feature points as measured by image processing. The coordinate of the feature point and the position and attitude of the vehicle calculated by the direct geo-referencing method are fed into the offsetting function of the Kalman filter and subject to a LOS calculation for SLAM.

3.3 System error model for SLAM Kalman filter

Vision-based SLAM is a method that estimates the position of a vehicle (localization) and creates a map (mapping) simultaneously for an unknown environment. In this paper, the position of the vehicle is estimated using the feature point in the downward-looking image and then updating the information of the map. Hence, in the first acquired image frame, the estimated position and attitude of the vehicle are used as the input to direct geo-referencing to create the map of each feature point (localization). In the subsequently acquired image frame, the position of the moving vehicle is updated using the coordinate of the feature point determined in the previous frame, and the coordinate of newly added feature point is then estimated with the newly estimated position of the vehicle (mapping).

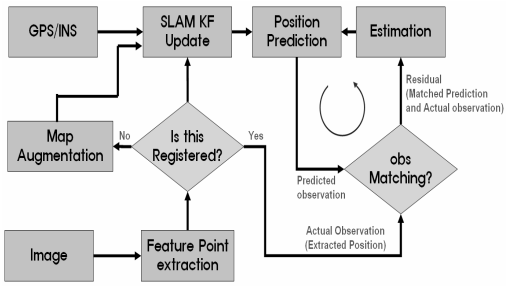

Fig. 7. Flow of the proposed SLAM Algorithm.

These processes are performed repeatedly, as depicted in Fig. 7.

The error model consists of position, attitude and velocity of vehicle, accelerometer and gyro bias, and map error. $\delta x(t)$ is error state vector, $F(t)$ is system state matrix, $G(t)$ is system noise input matrix and $w(t)$ is system input noise vector.

$$\delta x(t+1) = F(t)\delta x(t) + G(t)w(t) \tag{2}$$

$$\delta x(t) = [\delta x_v(t), \delta x_i(t), \delta x_m(t)]^T \tag{3}$$

$$\delta x_v(t) = [\delta p^n(t), \delta v^n(t), \delta \psi^n(t)]^T \tag{4}$$

$$\delta x_i(t) = [\delta f(t), \delta \omega(t)]^T \tag{5}$$

$$\delta x_m(t) = [\delta m_1^n(t), \delta m_1^n(t), \cdots\cdots, \delta m_N^n(t)]^T \tag{6}$$

$$\begin{bmatrix} \delta p^n \\ \delta v^n \\ \delta \phi^n \\ \delta m_m^n \end{bmatrix} = \begin{bmatrix} \delta v^n \\ C_b^n f^b \times \delta \psi^n + C_b^n \delta f^b \\ -C_b^n \delta \omega^b \\ 0_m \end{bmatrix} \tag{7}$$

where δf^b is the measurement error of IMU, and C_b^n is the DCM(Direct Cosine matrix) matrix between navigation and body frame.

3.4 Measurement model

Position compensation

The position information determined by direct geo-referencing is fed back into the input of Kalman filter, and it updates the error information.

$$\begin{aligned} z &= P_{gps/ins} - P_{georeferencing} = P_{gps/ins} \\ &-(C_b^n C_m^b (r_i^m(t) + C_b^m(t)(s_p \cdot C_c^b \cdot r_p^c - a_{INS}^c - a_{INS}^{GPS})) \end{aligned} \tag{8}$$

Line of sight vector

The attitude measured by INS is fed to the input coefficient of the direct geo-referencing and it leads to the navigation solution. Therefore if there are some measurement errors in

the attitude output, they influence the navigation solution directly. To prevent such attitude measurement error, we use the LOS vector to compensate for the position as well as the attitude of vehicle.

In detail, we derive the residual for two LOS vectors. One is the gimbal angle vector from the forward-looking image and inertial sensor, which is the direction of view point from the vehicle to the target feature point. The other is the positioning angle vector between the vehicle and the target position [15].

$$\begin{aligned} z &= \hat{e}^n_{landmark} - \hat{e}^n_{gimbal} \\ &= [e^n_{landmark} + \delta e^n_{landmark}] - [e^n_{gimbal} + \delta e^n_{gimbal}] \\ &= \delta e^n_{landmark} - \delta e^n_{gimbal} \end{aligned} \tag{9}$$

Range between vehicle and feature point

To obtain the measurement equation for the range between the vehicle and the *i*-th feature point on the earth surface, we use the location of the point vector (r^c_p) in the image frame of the direct geo-referencing equation.

$$r^c_p(k) = \begin{bmatrix} \rho\cos(\phi)\cos(\vartheta) \\ \rho\sin(\phi)\cos(\vartheta) \\ \rho\sin(\phi) \end{bmatrix}, \quad \begin{bmatrix} \rho \\ \phi \\ \vartheta \end{bmatrix} = \begin{bmatrix} \sqrt{x^2+y^2+z^2} \\ \tan^{-1}(y/x) \\ \tan^{-1}(z/\sqrt{x^2+y^2}) \end{bmatrix} \tag{10}$$

3.5 Image processing

One of the important factors in vision-based SLAM involves precisely extracting the coordinate of the image for the tracking of the feature points in image frames. The navigation algorithm serves to compare the extracted image coordinate and the estimated point of the Kalman filter. Fig. 8 describes the process of image processing. Given that the raw input image has noise as well as image information, it is not possible to use the feature point extraction directly. Therefore, to remove the impulse noise elements and preserve the robust edge at the same time, a median filter is used instead of a low-pass filter. This generally removes the Gaussian noise.

During the stage of feature detection, it is necessary to extract all feature points above a predefined threshold level to guarantee robust matching in spite of the serious disturbance due to the noise in the raw images. In this study, we use the Harris corner and SIFT method to compare each pixel on the outskirts [16].

During the matching stage, the extracted feature points in each image become linked from frame to frame. These linked feature points in the current image indicate the direction in the next image. Thus, the movement of the vehicle and the camera can be estimated using this information. The corresponding points can be found by comparing the intensity values in local windows with various matching metrics. In this paper, the SSD(sum of squared distance) method is used.

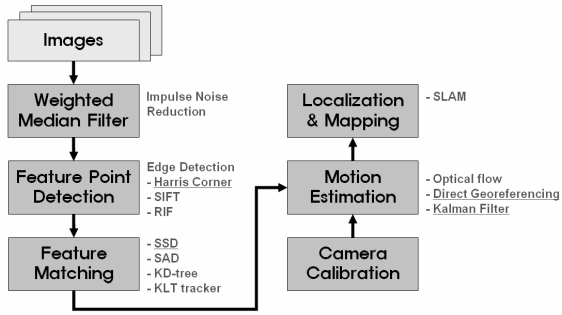

Fig. 8. Flow of image processing for SLAM.

The image-processing method for SLAM proceeds as follows. The total number of feature points should be limited in real-time processing; and these points should be equally placed over all sectors of the image. The feature point that is the position reference should be selected with the highest correlation value.

4. Test and evaluation

To evaluate the GPS/INS/vision navigation system, the flight tests were conducted four times. The GPS antenna and two cameras were installed on the exterior of the helicopter. The tactical information display device was installed at the cockpit frame for a pilot to evaluate the coincidence of the artificial vision. Also, the navigation system and tactical information processor were installed on the cabin to collect the data for the evaluation.

4.1 Test scenario

For the evaluation of the effectiveness of multi-vision-based GPS/INS navigation, the test area is divided into three test areas: a forward-looking-only area, a downward-looking-only area and a forward-downward-looking integrated navigation area, as shown in Fig. A.1.

Forward-looking only: ⓑ～ⓓ area

After take-off, the forward-looking-only integrated navigation was tested by blocking the GPS signal. As the helicopter was flying at a low altitude, it was not easy to obtain a sufficient FOV from the downward-looking image.

Downward-looking only: ⓕ～ⓖ area

The test area was located in the middle of a mountainous area. FOV of the forward-looking image was narrow, and it was impossible to detect the feature point in the image. However, with the downward image, it was possible to assess the navigation. Therefore, an analysis of the degree of the position compensation under navigation is planned.

Forward-downward-looking: ⓗ～ⓙ area

This area had adequate information in the forward and downward-looking image. The final navigation evaluation was performed by coupling the multi-vision sensor.

Fig. 9. Helicopter for the flight test.

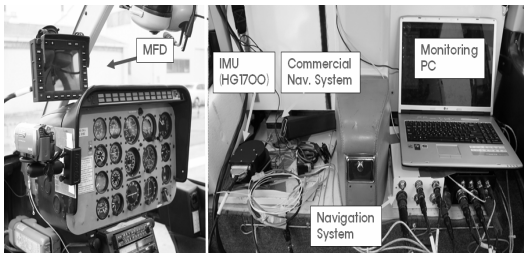

(a) Cockpit (b) Cabin

Fig. 10. Test apparatus inside the helicopter.

4.2 Test result

Flight tests were performed around the Daejeon area with Bell-206 helicopter, as shown in Figs. 9 and 10. For the reproduction of a GPS blockage situation due to a steep attitude change of the vehicle, the flight test scenario was planed to turn around a waypoint as quickly as possible, as shown in Fig. A.2.

Forward-looking only: ⓑ～ⓓ area

If the GPS signal is blocked, the keypoints are extracted in the forward-looking image from the SIFT method, as shown in Fig. 14. Many keypoints located in the area were used for the tracking image area, and the LOS vector of the keypoints was calculated using these points. As time passed, if the number of the matched keypoints decreased, the algorithm selected a new tracking image and keypoints in place of the previous tracking image. As for the results in the forward-looking integrated navigation, there was little divergence, as in GPS/INS, but the navigation solution moved back and forth slightly. The error sources were inferred by the LOS vector estimation and distance calculation between the position of the helicopter and the landmarks.

Downward-looking only: ⓕ～ⓖ area

In the flight test, GPS signal blockage occurred around the waypoint for 1 minute when the roll angle ranged from 0° to -20° and the yaw angle ranged from +150° to -50°. At that time, the average flight ground speed was 110 knots. In the GPS/INS navigation, the error level was within 320 meters from the reference track after GPS signal blockage occurred; however, in the GPS/INS/Vision navigation(refer to Fig. A.5.), the error level was improved within 20 meters. Especially when the LOS from the forward-looking camera was available, the error in the navigation solution showed a considerable decrease.

Table 3. Flight test result of GPS/INS/vision navigation.

Flight Test (B-206)		Position Error (m)		
		N	E	D
GPS/INS /Vision	AVR	1.0898	0.4857	-0.5593
	RMS	0.7415	1.4659	1.9192

Forward-downward-looking: ⓗ～ⓙ area

The result of this area was that the trembling in this direction decreased when using the distance variation of the downward-looking image; this is the weak point of the forward-looking-only navigation. The divergence in the downward-looking-only navigation was also decreased when using the LOS vector of the forward-looking image.

4.3 Evaluation

Due the limited payload and electric power capacity of the helicopter, the precise reference system (MAPS INS) could not be mounted. Instead, the post-processing DGPS was used to evaluate the performance and consistency. The test results in Table 3 show that the accuracy of the vision-based GPS/INS navigation system meets the CAT-I requirements. There are a few differences between the GPS/INS and GPS/INS/vision schemes in terms of accuracy under general conditions. However, under high multipath and GPS signal blockage conditions as shown in Fig. A.3., the GPS/INS/vision navigation system performed more robustly, compared to the GPS/INS navigation system.

Using the pathway-in-the-sky view generated from the ground control system, it was possible to fly to Mt. SikJang safely, even in low visibility conditions such as fog, haze or cloudiness.

5. Conclusions

The proposed navigation system is for a helicopter and it can handle rugged operation environments. Owing to the high speed, steep attitude variance, and rotor of the helicopter, GPS signal blockage and attenuation occurred frequently. Therefore, in addition to GPS to offset the INS error, a vision sensor coupled with a GPS/INS navigation system was developed.

Flight tests were carried out to evaluate the overall system performance of the vision-based GPS/INS navigation system that provides an artificial view with the multi function display. The experimental results show that the proposed navigation system is effective such that compared to the GPS/INS navigation system, it does not lead to a divergence of the navigation solution, particularly in poor operations characterized by GPS signal blockage and multipath.

Future work is needed to develop a vision-based GPS/INS navigation system with synthetic vision in an effort to improve the accuracy of navigation and the situational awareness in various environments.

Acknowledgment

This study was financially supported by research fund of Chungnam National University in 2009.

References

[1] R. P. G. Collinson, *Introduction to Avionics*, Chapman & Hall, (1996).

[2] G. Brodin, J. Cooper and D. Walsh, The effect of helicopter rotors on GPS signal reception, *The Journal of Navigation*, 58 (3) (2005) 433-458.

[3] A. Wu and E. Johnson, A. Proctor, Vision-aided inertial navigation for flight control, *Proc. of Guidance, Navigation, and Control Conference,* AIAA 2005-5998*,* San Francisco, USA, (2005).

[4] T. Templeton and D. H. Shim, et al. Autonomous vision-based landing and terrain mapping using an MPC-controlled unmanned rotorcraft, *Proc. of IEEE International Conference on Robotics and Automation(ICRA)*, (2007) 1349-1356.

[5] J. Kelly, S. Saripalli and G. Sukhatme, Combined visual and inertial navigation for an unmanned aerial vehicle, *Proc. of the International Conference on Field and Service Robotics*, France, (2007) 255-264.

[6] D. G. Lowe, Distinctive image features from scale-invariant keypoints, *International Journal of Computer Vision*, 60 (2) (2004) 91-110.

[7] C. Harris and M. Stephens, A combined corner and edge detector, *Proc. of the Fourth Alvey Vision Conference*, Manchester, UK, (1988) 147-151.

[8] S. Ettinger and M. Nechyba, et al., Vision guided flight stability and control for micro air vehicles, *Proc. of IEEE International Conference on Intelligent Robots and Systems*, Switzerland, 3 (2002) 2134-2140.

[9] W. E. Green and P. Y. Oh, et al., Autonomous landing for indoor flying robots using optic flow, *Proc. of ASME International Mechanical Engineering Congress*, Washington, D.C., USA, (2003) 1347-1352.

[10] J. H. Kim and S. Sukkarieh, Airborne simultaneous localization and map building, *Proc. of IEEE ICRA*, Taipei, (2003) 13-29.

[11] *MPC8560 Reference Manual*, Freescale Inc., (2003).

[12] M. Duchaineau and M. Wolinsky, et al., ROAMing terrain: real-time optimally adapting meshes, *Proc. of IEEE Visualization*, Pheonix, USA, (1997) 81-88.

[13] A. K. Barrows, K. W. Alter, C. J. Jennings and J. D. Powell, Alaskan flight trials of a synthetic vision system for instrument landings of a piston twin aircraft*, Enhanced and synthetic vision, SPIE*, Orlando, USA, (1999) 98-107.

[14] El-Sheimy, The development of VISAT: a mobile survey system for GIS applications, *UCGE Report #20101,* Dept. of Geomatics Eng., University of Calgary, Canada, (1996).

[15] S. J. Oh and W. H. Kim, Design of INS/image sensor integrated navigation system, *Journal of Control, Automation, and Systems Engineering*, 12 (10) (2006) 982-988.

[16] M. Cramer, D. Stallmann and N. Haala, Direct georeferencing using GPS/inertial exterior orientations for photogrammetric applications, *International Archives of the Photogrammetry, Remote Sensing and Spatial Information Sciences*, Amsterdam, 33 (B3) (2000) 198-205.

Appendix: Flight test results

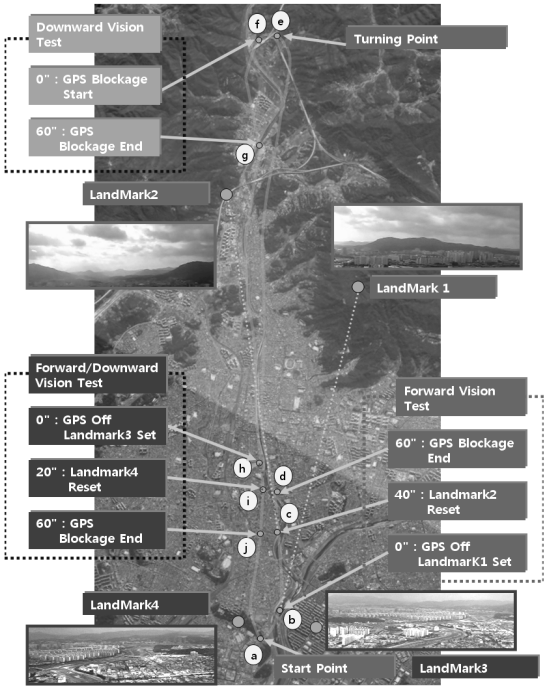

Fig. A.1. Flight course and test condition.

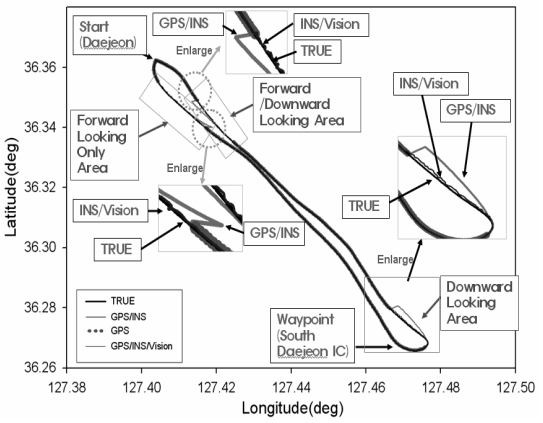

Fig. A.2. Comparison of the navigation schemes.

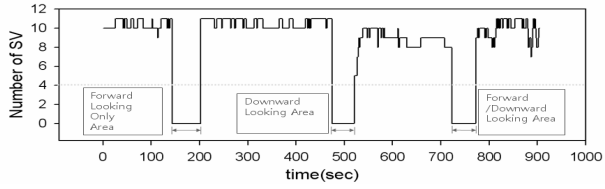

Fig. A.3. Number of satellites visible.

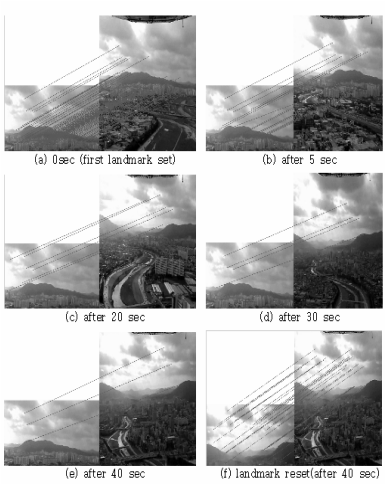

Fig. A.4. Forward-looking image processing by SIFT.

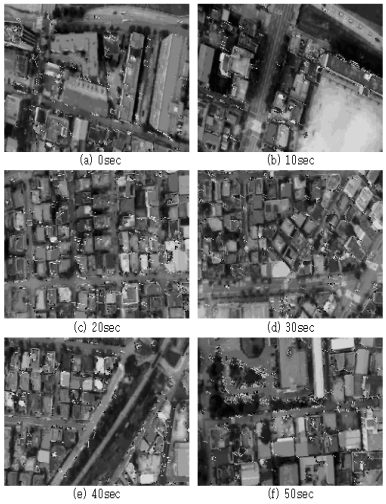

Fig. A.5. Downward-looking image processing by Harris corner.

JaeHyung Kim received the B.S., M.S. and Ph.D in Electronics Engineering from Chungnam National University in 1995, 1997 and 2008, respectively. Dr. Kim is a principal researcher of Korean Air R&D Center. His research interests include avionics, navigation system, embedded system, and control systems.

Joon Lyou received a B.S. in Electronics Engineering from Seoul National University in 1978. He then went on to receive M.S. and Ph.D. degrees from KAIST in 1980 and 1984, respectively. Dr. Lyou is currently a professor of the Department of Electronics Engineering at Chungnam National University in Daejeon, Korea. His research interests include industrial control and sensor signal processing, IT based robotics, and navigation systems.

HwyKuen Kwak received a B.S. in Electronics Engineering from Chungnam National University in 2005. He is currently working on his M.S. and Ph.D. course at Chungnam National University in Daejeon, Korea. His research areas are image signal processing, sensors and digital control systems.